

IoT Motion Tracking System for Workout Performance Evaluation: A Case Study on Dumbbell

Shilong Sun^{ID}, Member, IEEE, Tengyi Peng^{ID}, Haodong Huang^{ID}, Yufan Wang, Member, IEEE, Xiao Zhang^{ID}, Member, IEEE, and Yu Zhou^{ID}, Member, IEEE

Abstract—An intelligent sports training system based on Internet of Things (IoT) technology is proposed to build a low-cost, easy-to-use home exercise guidance solution, which can provide reliable exercise guidance when gyms are inaccessible for users. The proposed intelligent system includes an inertial measurement microelectromechanical system with Bluetooth low-energy data transmission technology, a smart dumbbell with an acceleration sensor, an application on the smartphone terminal, and a computing central server in the clouds. Two-loop Kalman filters, dynamic motion segmentation method, and neural network are developed to demonstrate and evaluate the user's dumbbell exercise modes. Six dumbbell exercise postures and 10 exercise cycles for eight participants are collected for system validation in the experimental study. The experimental results demonstrate that the proposed system can effectively and accurately segment multiple types of dumbbell movements (98.9% accuracy), recognize movements with high reliability (98.3% accuracy), and distinguish standard and non-standard movements (89% accuracy). Finally, this system with an intelligent algorithm software and hardware can be expanded to other similar types of sporting excises.

Manuscript received 14 May 2023; revised 2 August 2023; accepted 22 September 2023. Date of publication 28 September 2023; date of current version 21 February 2024. This work was supported in part by the Natural Science Foundation of Guangdong Province under Grant 2021A1515110615; in part by the National Natural Science Foundation of China (NSFC) under Grant 61702336 and Grant 61902437; in part by the Shenzhen Fundamental Research Program under Grant JCYJ20220810112354002 and Grant JCYJ2020010911041013; in part by the Fundamental Research Funds for the Central Universities; in part by the South-Central Minzu University under Grant CPT22017; in part by the Research Start-Up Funds of South-Central Minzu University under Grant YZZ18006; in part by the Knowledge Innovation Program of Wuhan-Basic Research under Project SZY23001; and in part by the Teaching-Research Program of National Ethnic Affairs Commission of China. (Corresponding author: Xiao Zhang.)

Shilong Sun, Tengyi Peng, and Haodong Huang are with the School of Mechanical Engineering and Automation, Harbin Institute of Technology (Shenzhen), Shenzhen 518055, China, and also with the Guangdong Provincial Key Laboratory of Intelligent Morphing Mechanisms and Adaptive Robotics, Shenzhen 518055, China (e-mail: sunshilong@hit.edu.cn; 20s053007@stu.hit.edu.cn; hhd1340201839@163.com).

Yufan Wang is with the Department of Industrial Engineering and Management, School of Mechanical Engineering, Shanghai Jiao Tong University, Shanghai 200240, China (e-mail: elvis@aimotionsports.com).

Xiao Zhang is with the Department of Computer Science and the Key Laboratory of Cyber-Physical Fusion Intelligent Computing, State Ethnic Affairs Commission, South-Central Minzu University, Wuhan 430074, China (e-mail: xiao.zhang@my.cityu.edu.hk).

Yu Zhou is with the College of Computer Science and Software Engineering, Shenzhen University, Shenzhen 518060, China, and also with the Key Laboratory of Cyber-Physical Fusion Intelligent Computing, State Ethnic Affairs Commission, South-Central Minzu University, Wuhan 430074, China (e-mail: yu.zhou@szu.edu.cn).

Digital Object Identifier 10.1109/TCE.2023.3320183

Index Terms—Motion tracking, exercise mode identification, posture evaluation, data stream segmentation, IoT technique.

I. INTRODUCTION

MEDICAL research has shown that physical exercise can help maintain physical health, reduce the risk of cardiovascular disease, obesity, stroke, and cancer, and improve the musculoskeletal health and stress regulation [1] as well as maintain mental health and reduce the risk of mental illness [2]. In July 2021, China launched the National Fitness Plan (2021–2025), which mentions “*Implementing the youth physical activity promotion plan, promoting the youth sports’ health package’ project, carrying out sports interventions for youth myopia, obesity, and other problems,*” and attaching importance to providing intelligent services for national fitness,” developing timely information dissemination, convenient services access, and an efficient information feedback system with a national fitness wisdom service mechanism. Fitness wisdom service requires the collection of information obtained from various sensors for automatic motion detection and analysis. Athletically identifying and analyzing sports movements is a remarkable direction in fitness wisdom services.

Many researchers have now researched human motion recognition [3], focusing on human motion behavior changes and fall monitoring to achieve intelligent medical rehabilitation and reduce reliance on manual labor [4]. For example, Zhou et al. [5] studied a neural network (NN)-based approach for human activity recognition. Arsenault and Whitehead [6] examined gesture recognition algorithms that use an inertial sensor worn on the forearm and this recognition algorithms use the sensor’s quaternion orientation in either a Hidden Markov Model or Markov Chain based approach. Al-Hammadi et al. [7] propose an efficient system for automatic hand gesture recognition based on deep learning. The proposed system is based on a convolutional neural network (CNN) and employs a transfer learning of 3D CNN for hand gesture recognition. Panella and Altilio [8] proposed a smartphone-based application using machine learning for gesture recognition which using feature extraction and template matching via hu image moments to recognize gestures. Ayata et al. [9] use a wearable device integrated with galvanic skin response (GSR) and photo plethysmography (PPG) physiological sensors to solve the emotion recognition problem.

Mortazavi et al. [10] built a game that utilizes wearable sensors to monitor the gamer to prevent sedentary behavior in childhood/adult obesity. Smerdov et al. [11] combined various sensors, including inertial sensors, to monitor the fatigue state of e-sports athletes, simultaneously preventing long-time athletic work fatigue. The fatigue of athletes is prevented by long hours of athletic work while aiding athletes in athletic decision-making. Likewise, motion analysis is required for fitness smart services. Dizon-Paradis et al. [12] proposed a flexible, reconfigurable human body movement and health monitoring platform, called “Pasteables”. Huang and Bai [13] studied the intelligent sports prediction analysis systems based on particle swarm optimization algorithm. For example, swimming postures recognition and analysis has received the attention of many researchers. Ganzevles et al. [14] investigated the application of three-axis acceleration sensors in swimming motion monitoring and recognition. Wang et al. [15] studied multiposition human swimming posture monitoring based on multisensor fusion for achieving accurate guidance during exercise. Dadashi et al. [16] studied wearable sensors regarding mechanical monitoring of swimming to detect the two different motions of freestyle and breaststroke. Additionally, Yoga care is also investigated by Yoga-hand mudra (hand gestures) identification [17]. The YOGI dataset has been developed which include 10 Yoga postures with around 400-900 images of each pose and contain 5 mudras for identification of mudras postures. Therefore, more and more sport exercises are combined with the state-of-art artificial intelligence algorithm to make them more smart and more efficient.

Although human motion recognition with wearable devices has been widely studied [3], all current devices have their limitations, mainly, the classification of executive motions or the accuracy analysis of actions, and few studies integrate the two aspects. Moreover, many studies do not involve the accurate motion segmentation of the sensor’s data stream. The goal of intelligent sports training is the same as telemedicine, connecting the users beyond the gym and coaches. To make intelligent fitness services meet the client’s requirements and reduce the cost of devices, the sensor devices and IoT systems require designed miniaturization and lightweight. Additionally, the sensors embedded in the IoT systems need a simpler, faster, and more functional algorithm. In 2014, Bulling et al. [18] provided a tutorial on traditional machine-learning methods for human motion recognition based on wearable inertial sensors. Afterward, Burns et al. [19] demonstrated that smartwatch devices and supervised machine learning methods can easily monitor and evaluate the effective execution of shoulder physical therapy home exercise programs. Based on wearable sensors, Kos and Umek [20] proposed a rehabilitation training framework with equal emphasis on local and remote diagnosis and treatment, which supports users to obtain feedback from local algorithms and timely attention of remote diagnosis and treatment personnel in training. Additionally, similar technologies have been introduced into fitness intelligent services. Hsu et al. [21] proposed a wearable system, which uses two wearable inertial sensing modules on athletes’ wrists and ankles to collect motion signals, and then designed a convolutional NN to extract inherent features from the short-term Fourier transform spectrum of motion signals

and realizes effective motion recognition in a variety of different movements. Sha et al. [22] integrated the acceleration sensor into the smart wristband to monitor and judge the accuracy of the recognized posture of table tennis. Ravi et al. [23] combine the spectrum feature extraction method with deep learning approach to build up an on-Node sensor data analytics method for wearable device motion recognition. Based on the sensor data, segmentation of the data is required before sending it to the motion analysis model [24] for motion segmentation. An effective method of motion segmentation is to set the time sliding window to segment the signal and intercept the data through the preset fixed-length sliding window. For example, the literature [25], [26] used the fixed-length sliding window for motion segmentation. Another method is to realize motion segmentation and anomaly detection through the analysis of data flow according to the pseudo periodicity of human motion behavior [27]. For complex situations involving multilimb movements, Hu et al. [28] cut and segmented motions through different semantic feature motions through intelligent semantic analysis. However, in the case of wearable device sensors, segmentation is mostly based on the waveform pseudo periodic characteristics of the motion data stream. Tang et al. [29] analyzed the peak and trough characteristics of the pseudo periodic signal to segment the signal, which is simple and effective. In the previous research [30], [31], based on the wearable device Internet of Things (IoT) system, the information on badminton movement was analyzed and processed, which realized the effective motion classification and greatly reduced the requirements of traditional motion monitoring for precision equipment. Moreover, Lu et al. [32] proposed a new AIoT (AI + IoT) paradigm for next-generation foot-driven sports (soccer, football, and takraw) training and talent selection. Therefore, wearable sensors and IoT technology play an essential role in motion tracking system design, especially for the intelligent sport training system.

As we all know, dumbbell exercise can stimulate muscles well to achieve exercise effect, and it is more convenient to do exercise, which is very suitable for professional and non-professional daily training [33]. However, most people’s movements are not standard when doing dumbbell exercises, and the effect of exercise is very low, which is not conducive to accurately grasping the exercise situation. Therefore, precise standardized training for dumbbell exercise movements is very necessary to be studied. Wearable sensors and IoT technology play an important role in intelligent sport. The development of artificial intelligence and the Internet of Things technology has realized the digitalization and intelligence of many traditional physical exercise projects, like dumbbell projects. Intelligent dumbbells that combine artificial intelligence and Internet of Things technology can effectively solve the above-mentioned two problems: 1) non-standard movements; 2) Low efficient workouts.

In this work, an intelligent dumbbell motion recognition and evaluation system, which uses a low-power microprocessor sensor with low-power Bluetooth technology and cloud technology, is proposed. This system demonstrates the possibilities of next-generation IoT sports devices using IoT. The techniques in this system can segment the signal for dumbbell movement type, classify the movement, and judge whether

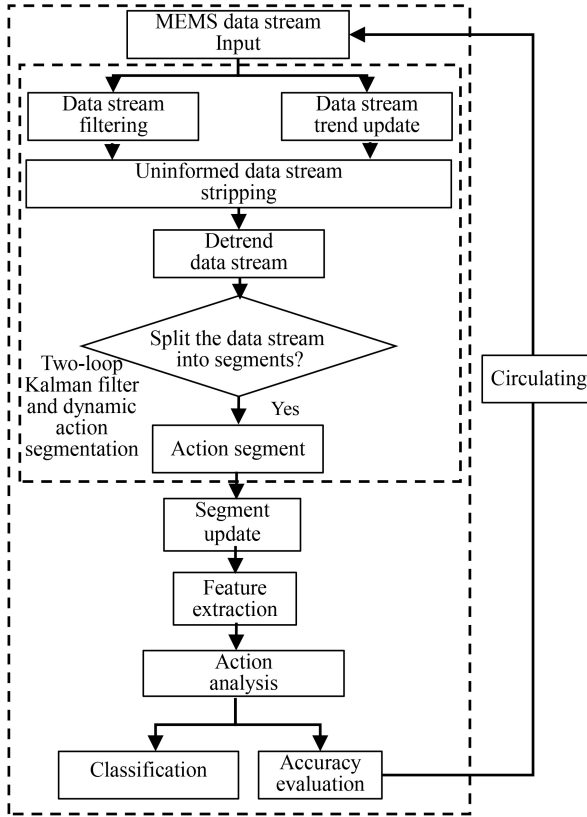


Fig. 1. The proposed dumbbell data stream processing algorithm.

the movement is standard. First, a wireless sensor device is developed and built into the dumbbell to collect inertial data. Second, a smartphone mobile application, which can visualize the experimental results, perform motion analysis, and upload the data from the experiment to the cloud server, is designed. Third, motion segmentation, motion classification accuracy, and NN algorithm are implemented in the cloud computing platform design. Fourth, a real case study is performed to demonstrate the reliability and validity of the whole system, including the software and hardware. It indicates that the overall system is capable of achieving effective automatic dumbbell exercise training guidance.

The rest of this paper is organized as follows. Section II gives the literature review. Section III introduces the hardware intelligent workout system and the dumbbell case study experiment setup. Section IV presents the algorithms of the motion segmentation and analysis. Section V shows the experimental study of the proposed system, and Section VI summarizes this work.

II. PROPOSED SYSTEM SCHEME

A. Intelligent Exercise System Workflow

The workflow of the system is shown in Fig. 1. The microelectromechanical system (MEMS) installed on the intelligent dumbbell is used to collect motion data and communicate with the host computer. In this paper, the microcomputer motor system collects the motion data of the acceleration of upper

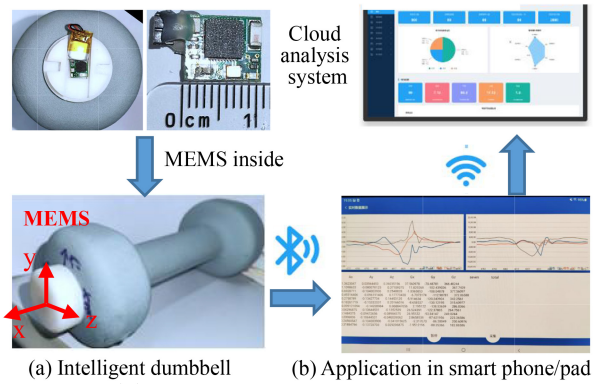


Fig. 2. Overview of MEMS data acquisition systems.

limb motion from six types of dumbbells. Through the two-loop Kalman filter and dynamic segmentation method, the dumbbell information is preprocessed, and motion segmentation is realized. After the motion segmentation is completed, the segmentation results are uploaded to the terminal. In the terminal, the time domain and frequency domain characteristics of the motion signal segment are extracted and input into the NN to realize motion classification and motion evolution and guide the user to exercise effectively.

B. MEMS Data Acquisition System

1) *Example of Wireless Inertial Measurement Sensing Unit and Arrangement:* Fig. 2 shows the initial design of the wireless inertial measurement unit. It consists of a microprocessor with a Bluetooth wireless communication module and a MEMS motion-sensing chip (with three-axis accelerometer) processor DA14583 (Dialog Semiconductor, Reading, U.K.) with Bluetooth integrated low-power radio transceiver platform. The MEMS system is built into the smart dumbbell.

The three-axis angular acceleration sensor is flatly attached to the center of one end of the dumbbell rod to realize the information acquisition of the dumbbell motion. When the dumbbell is placed horizontally on the ground, the x-axis of the inertial sensing should be vertical to the horizontal plane, the y and z axes are parallel to the horizontal plane, and the x and y axes form a plane parallel to the dumbbell piece, as shown in Fig. 2(b).

2) *Software Interaction System:* Since the MEMS DA14583 has limited computational power and the smart terminal can provide more motion guidance to users, an intelligent mobile motion application is designed. The function of this application concludes the motion signal feature extraction and motion analysis, intelligent decision-making, etc. Fig. 3 shows the technical implementation method. The whole system consists of three parts: wearable smart Bluetooth sensing device, mobile terminal and cloud server. The entire system process is to use the raw motion data through the wearable MEMS sensor and then transmit it to our intelligent management cloud. After receiving the data, the cloud uses artificial intelligence algorithms to evaluate their posture and give real-time feedback. This mobile application uses the Evothings framework, which is used to create IoT mobile

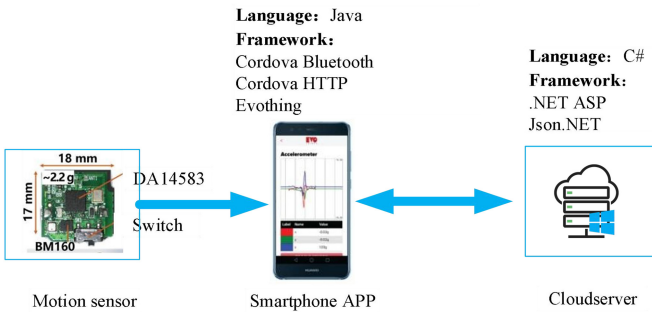


Fig. 3. Technical implementation method.

development applications. The open-source framework is based on the JavaScript programming language. The software system consists of a low-power Bluetooth module, sensor data display, and motion analysis module. The low-power Bluetooth module is based on Evothings and Cordova BLE plug-ins and enables low-power Bluetooth support for Android, iOS, and Windows. A cloud backend system that automatically uploads data to the cloud when mobile devices receive it and is also built by our system. The Cordova HTTP plug-ins are used to implement the upload and save functions.

C. Experimental Scheme

In this paper, six dumbbell movements are selected as the experimental dumbbell movements for signal acquisition and analysis, namely, single-arm row, single-arm stretch behind the neck, curls, side planks, dumbbell bench press, and bench flyer. These six motions are briefly introduced as follows:

1) *Single-Arm Rowing*: The upper body is tilted forward and fixed, the abdomen is closed, the chest is raised, and the waist is straight. During the exercise, the arm is close to one side of the body and pulled up to the limited position of the highest point, feeling the latissimus dorsi fully tightened. After a short stay at the highest point for 2–4 s, it slowly falls to the vertical position between the large arm and the ground, and the elbow is slightly bent.

2) *Single-Arm Neck Posterior Arm Flexion and Extension*: The right-hand holds the bell, palm forward, and straight above the head. The left hand is held on the left wrist, and the right upper arm is kept close to the right ear. No movement is made. The dumbbell falls to the top of the left shoulder in an arc; the lower it is, the better. Then, the bell is held and lifted with the contraction force of the triceps brachii of the right arm.

3) *Dumbbell Curl*: The elbow joint is taken as the fulcrum and bent upward. The forearm is rotated outward with the palm facing upward and lifted to the highest point. The bicep brachii are tightened, and movement is stopped for a while. The main exercise part is the bicep brachii. The critical point of the motion is that the forearm rotates outward, the palm is upward during the bending lift, and the arm cannot be straightened during the relaxation.

4) *Side Lateral Raise*: Both hands grip the dumbbells on both sides of the body, elbows are slightly bent, and fist eyes are forward. Both hands hold the bell simultaneously to both sides of the lift so the upper arms can be parallel to the ground

and then slowly fall back to the original position in the same way. The main exercise parts are for the deltoids. The key to motion is not to fling during the side planks up to the upper arms parallel to the ground.

5) *Dumbbell Bench Press*: Lying flat on the mat, the dumbbells are kept in front of the chest, pushed up, lowered to the same height as the chest, and pushed up again to the original position. The process is repeated. The exercise areas are the pectoralis major, deltoids, and triceps. The critical points of the movement are to avoid straightening the arms completely, and the lowest point should be slightly above the chest.

6) *Dumbbell Bench Flying Bird*: The upper back and hips touch the bench surface when lying on the bench and with firm feet on land. The dumbbells of both arms naturally extend directly above the shoulder joint, and the distance between the hands is slightly less than the shoulder width. Two arms holding the dumbbells fall to the side of the body slowly. In falling, the angle between the elbows gradually decreases, and the elbow joint forms an angle of 100°–120° at the limit. The pectoralis major muscle contracts and raises the dumbbell along the original path. The rising route is “arc,” and the angle between elbows increases gradually. The critical point of the motion is that the shoulder, elbow, and wrist joints are in the same plane during the whole motion.

The six motions are shown in Fig. 4. Experimental data are collected from eight different participants. Before starting the data collection, they are invited to pre-train under the guidance of a professional physical fitness trainer until they fluently complete the movements. Then, ten effective repetitions of each movement are completed. Each individual's actions are collected consistently, and the duration of each action varies from 1 s to 3 s depending on the motion and the participant's strength. The signals are obtained from the built-in MEMS sensor of the dumbbell held in the right hand.

III. TWO-LOOP KALMAN FILTERING WITH DYNAMIC MOTION SEGMENTATION

This Section mainly introduces the real-time microprocessor processing, low-arithmetic-power requirements, and simple computation that can be used simultaneously for all six dumbbell motions. For achieving motion segmentation, measured signal filtering and detrend are necessary. We have designed a Kalman filtering algorithm for signal filtering and real-time detrending and proposed a two-loop Kalman filtering algorithm. The flow chart of the two-loop Kalman filtering algorithm is shown in Fig. 1.

A. Datastream Filtering

Datastream filtering includes smoothing filtering and real-time stripping of uninformative signals. Smoothing filtering is to remove the influence of environmental noise and sensor noise in sensor acquisition, and no-information signal real-time stripping can reduce the influence of invalid information on signal analysis. It also reduces the amount of data transfer in the information transfer and improves analysis efficiency.

1) *A Signal Smoothing Filtering Algorithm*: Assuming that the acceleration measurements obtained for each axis obey

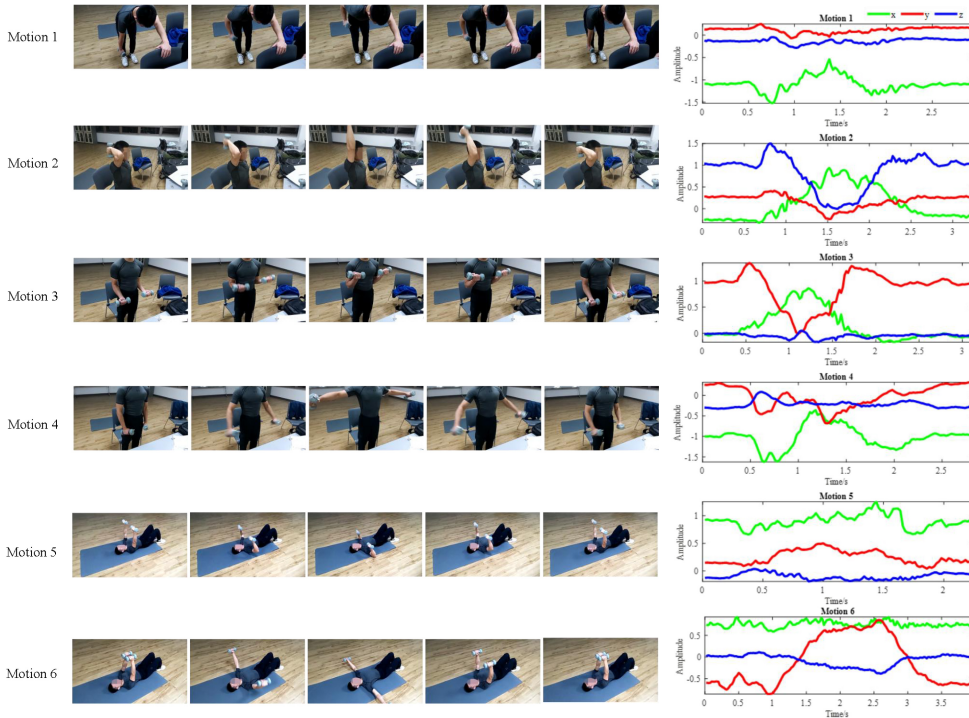


Fig. 4. The motion captures and their signals in the XYZ-axis.

a Gaussian probability distribution, for example, the x-axis acceleration observed by the sensor at time t satisfies $a_x^t \sim N(\bar{a}_x^t, \sigma_x^t)$, then all the data $X^t = (a_x, a_y, a_z)^T$ observed by the sensor at the time t obey a joint Gaussian probability distribution $N(\hat{X}^t, C^t)$, and C^t is the covariance matrix of the joint probability distribution at the time t . The expected \hat{X}^t is the filtered data stream result, which is used for subsequent analysis. To simplify the calculation, the first-order model is used to deduce the state transition of the joint Gaussian distribution, that is, $\bar{X}^{t+1} = F\hat{X}^t = Z^{t+1} = H\bar{X}^{t+1}H^T$, in which F, H are the state transition matrix and the observation matrix respectively, which are the unit matrices; Z^{t+1} is the sensor observation value according to the predicted time $t + 1$; \bar{X}^{t+1} is the a priori expectation of the joint probability distribution at time $t + 1$ obtained from the joint probability distribution at time t .

Assuming that the posterior joint probability density at moment t is $N(\hat{X}^t, C^t)$, the $N(\hat{X}^{t+1}, C^{t+1})$ procedure for deriving the posterior joint probability density at moment $t+1$ using signal smoothing with Kalman filtering is divided into the following steps.

1. The predicted joint probability density $N(\hat{X}^{t+1}, C^{t+1})$ at moment $t+1$ is generated from the state transfer matrix F and process noise variance matrix QC , where $\bar{X}^{t+1} = F\hat{X}^t$, and $\bar{C}^{t+1} = FC^tF^T + QC$.
2. Kalman gain $K = \bar{C}^{t+1}H^T/(H\bar{C}^{t+1}H^T + RC)$ is calculated from the a priori results, where RC is the observed noise variance matrix.
3. The difference between the observed and predicted expected Z^{t+1} at time $t+1$ is calculated, and $\Delta = X^{t+1} - Z^{t+1}$.

4. The posterior joint probability density function $N(\hat{X}^{t+1}, C^{t+1})$ is updated for moment $t+1$, $\hat{X}^{t+1} = \bar{X}^{t+1} + K\Delta$, and $C^{t+1} = (I - KH)\bar{C}^{t+1}$.
5. The expectation of the a posteriori joint probability density $N(\hat{X}^{t+1}, C^{t+1})$ is recorded as the result after filtering at moment $t+1$.

For the initial power-on acquired signal $X^0 = (a_x^0, a_y^0, a_z^0)^T$, $\bar{X}^0 = X^0$, and the corresponding covariance matrix C^0 , the process noise variance matrix QC , and observation noise variance matrix RC are simultaneously generated.

2) *Real-Time Stripping of Uninformed Signals:* The real-time stripping of the noninformation signal is to add an elliptical gate in the iterative Step 5 mentioned in Section III-A. to judge whether the sensor observation value at time $t + 1$ can still be regarded as the joint probability distribution $N(\hat{X}^t, C^t)$ from time t . If it can be regarded as the probability distribution $N(\hat{X}^t, C^t)$ from time t , the result at time $t + 1$ is not recorded. Normalized distance d is used to describe the expected $N(\hat{X}^t, C^t)$ difference between the measured value of the sensor at time $t + 1$ and the probability distribution at t :

$$d = (X^{t+1} - \hat{X}^t)^T / C^t \times (X^{t+1} - \hat{X}^t) \quad (1)$$

Normalized distance d fits the t-distribution with 3 degrees of freedom. Therefore, a 95% confidence interval is selected as the elliptic threshold, that is, $d < 12.83$, the observation at moment $t+1$ is not recorded, and the data stream filtering iterative process with the addition of uninformative signal stripping in real time is then modified from iteration Step 5 in the previous Section as follows:

If $d \triangleq \Delta^T / C^t > 12.83$, then the expectation \hat{X}^{t+1} of the posterior joint probability density $N(\hat{X}^{t+1}, C^{t+1})$ is recorded as the result after filtering at moment $t+1$; otherwise, it is not recorded.

B. Data Stream Segmentation

The time required to complete a motion cycle varies greatly because different people perform dissimilar motions, so the fixed-length sliding window is unsuitable for motion extraction. For example, in the dumbbell reclining movement, the cycle length of completing a single movement is as long as 3s, whereas the single dumbbell flying bird movement takes only 1s. The difference in time length increases the difficulty of obtaining an effective movement through a single-length sliding window. Moreover, even if the same person makes the same motion, the length of each exercise cycle cannot be the same.

However, in the dumbbell movement, a single motion always moves for dozens of cycles, so the data stream collected by the sensor can be regarded as a pseudo-periodic data stream. The pseudo-periodic data stream has some characteristics [29]: 1) The data stream can be divided into multiple waves with similar duration. 2) The shapes of the data streams in adjacent waves are very similar. Therefore, the pseudo periodic data stream division method can be used to segment the data stream. Data stream segmentation includes two parts: the first part is to obtain the detrended signal, and the second part is to perform over-segmentation through the detrended signal.

1) Detrended Signal Acquisition Algorithm: To obtain the mean value that can accompany the signal in real time, $N(\hat{X}_m^t, C_m^t)$ is used to describe the Gaussian probability density function that is consistent with the mean value of the gyroscope sensor over a short period at moment t . Similarly, $N(\tilde{X}_m^t, C_m^t)$ is updated using the same Kalman filtering method. Process noise variance matrix QC_m and observation noise variance matrix RC_m are different from QC and RC above, scaling up observation noise matrix QC_m and scaling down process noise matrix RC_m , and enabling this loop Kalman filter to extract the real-time mean.

Similarly, the expected \hat{X}_m^t of $N(\hat{X}_m^t, C_m^t)$ at time t is considered the real-time mean of the signal, and the detrended signal can then be obtained by $\tilde{X}_m^t - \hat{X}_m^t$.

2) Motion Segmentation Based on Pseudo Periodic Features: The pseudo periodic signal of dumbbell motion is segmented by shape features. Considering the different acceleration waveforms of six motions, the graphic segmentation method is adopted [29]. The pseudo periodic data stream is composed of bands with different time lengths and values. The band starts and ends in the middle of the two peak points. Therefore, the data flow can be divided into several segments according to the peak point. Typically, the lower limit of the peak is pre-specified in the application. For example, in the x-axis acceleration data stream, if the value of the valley point is usually greater than 0.1, then 0.1 can be used as a threshold V_s . When the value of the detrending x-axis acceleration exceeds 0.1, this value is the distinguishing peak value point V that is used to produce signal segmentation. However, the

peak value may change with the development of the data flow. Therefore, the exponential average of the peaks collected in the past is used to maintain real-time updates:

$$V_s = \alpha V_s + (1 - \alpha)V \quad (2)$$

where α is set as 0.6 in this study. Considering the variation of the stream data values, a detecting threshold is introduced to activate peak value detection. The detecting threshold is set to $0.4V_s$, the algorithm will detect the new peak value V when the measured data is up than $0.4V_s$. A suitable detecting threshold can improve the flexibility of the algorithm. If detecting threshold is too small that it may generate many ineffective segmentations, whereas a larger detecting threshold leads to segmentation disability. Therefore, optimal detecting threshold is set to $0.4V_s$ empirically. Moreover, so that the x, y, and z-axis criteria do not interfere with one another when looking for peak or valley values, only the result of the axis with the largest absolute value of peak (valley) values is used as a criterion.

C. Motion Feature Extraction, Motion Classification, and Motion Accuracy Evaluation

Once the motion segmentation is completed, the MEMS system uploads the data segment information into the mobile application of the user terminal. The motion type is analyzed using an NN approach, and this step consists of two main parts, namely, motion feature extraction and motion classification.

1) Motion Feature Extraction: Motion feature extraction is divided into two parts, namely, time-domain signal features and frequency domain signal features, and the extracted time-domain signal features are shown in TABLE I above. Because the time-domain statistical features are computed directly from the raw accelerometer data captured in real time and are often more intuitive and easier to interpret than other signal representations.

Three frequency-domain features are extracted as a supplement to the motion signal features. Given that the signal length of each segmented motion signal segment is different, before extracting the time-domain features of the signal, each motion signal is linearly interpolated, the signal length is unified to 200 data points, and then the interpolated signal is standardized to make its variance and mean value 1, 0. Finally, the normalized signal is Fourier transformed to obtain the spectrum F. To keep each feature on the same order of magnitude, the spectrum coordinate f of Fourier transform is an increasing sequence of 0–10. The three time-domain characteristics are center of gravity frequency, mean square frequency, and frequency variance. The corresponding discrete formula is calculated as follows:

$$FC = \frac{\sum f \times F(f)}{\sum F(f)}, \quad (3)$$

$$MSF = \frac{\sum f \times F(f)^2}{\sum F(f)}, \quad (4)$$

$$VF = \frac{\sum (f - FC)^2 \times F(f)^2}{\sum F(f)}, \quad (5)$$

TABLE I
STATISTICS FEATURES IN TIME DOMAIN

Mean value	$\mu = \frac{1}{N} \sum_{i=1}^N X_i$
Standard deviation	$\sigma = \sqrt{\frac{1}{N-1} \sum_{i=1}^N (X_i - \mu)^2}$
Maximum value	$X_{\max} = \max(\mathbf{X})$
Minimum value	$X_{\min} = \min(\mathbf{X})$
Mean absolute deviation	$M = \frac{1}{N} \sum_{i=1}^N X_i - \mu $
Interquartile distance	$IQR = X_{0.75N} - X_{0.25N}$
Range	$R = X_{\max} - X_{\min}$
Skewness	$\text{Skew} = E \left[\left(\frac{\mathbf{X} - \mu}{\sigma} \right)^3 \right]$
Absolute mean value	$A = E(\mathbf{X})$
Crest factor	$C = \frac{R}{\sqrt{\frac{1}{N} \sum_{i=1}^N X_i^2}}$
Impulse factor	$I = \frac{R}{\frac{1}{N} \sum_{i=1}^N X_i }$
Form factor	$SF = \frac{\sqrt{\frac{1}{N} \sum_{i=1}^N X_i^2}}{\frac{1}{N} \sum_{i=1}^N X_i }$

In summary, each motion time series has 15 features, and the signal collected by the sensor contains x, y, and z data, so 45 features are used for the subsequent NN motion analysis.

2) *Motion Classification, Accuracy Evaluation Neural Network:* Considering that the network needs to be deployed on mobile applications, the structure of the NN needs to be relatively simple. Therefore, a simple network structure with seven layers is used in this paper to implement motion classification and pose accuracy assessment. The structure of the network is shown in Fig. 5, which contains two parts, namely, motion classifier and pose discriminator, which is multiclassification network structures. In pose identification, the motion pose is classified into three categories, namely, perfect, good, and bad, so that the user can directly judge whether the pose is standard by the motion pose accuracy assessment results, and forming a report to summarize the exercise results is convenient.

The detailed parameters of the network are shown in TABLE II below.

To judge the accuracy of the motion pose, in this paper, the dynamic time warping (DTW) [34] method is introduced to score the segmented completed data segments and classify the motion criteria levels in the following steps:

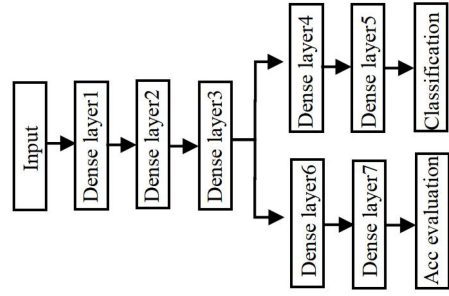


Fig. 5. Schematic diagram of the network structure.

TABLE II
NETWORK STRUCTURE DIAGRAM

Network structure	Dense	Activation function
Fully connected layer 1	128	Sigmoid
Fully connected layer 2	64	Sigmoid
Fully connected layer 3	32	Sigmoid
Fully connected layer 4	16	Sigmoid
Fully connected layer 5	16	Sigmoid
Fully connected layer 6	6	SoftMax
Fully connected layer 7	3	SoftMax

1. Demeaning of x, y, and z-axis information for all data segments is performed.
2. Two movement segments per movement are selected as standard templates from the data collected by the coaches.
3. For each motion segment, the DTW distance is calculated with the two standard template motion segments of its corresponding motion, and the mean value of the two DTWs is calculated as the motion scoring parameter.
4. According to the motion scoring parameters, a motion scoring parameter < 3 means the accuracy of the motion pose is perfect, 3 < motion scoring parameter < 6 means good, and 6 < motion scoring parameter means to be improved (bad). Finally, the label is generated.

Different weights are assigned to the sample classification labels in the training, considering the uneven distribution of classification labels in motion accuracy analysis. The higher the proportion of labels is, the smaller the weight to avoid the influence of label imbalance.

IV. ANALYSIS OF EXPERIMENTAL RESULTS

In this experimental analysis section, the two-loop Kalman filtering with dynamic motion segmentation is implemented, and the accuracy of motion segmentation is evaluated. In the motion classification and accuracy analysis, comparisons are made with the plain Bayesian, support vector machine (SVM), and k-nearest neighbor (KNN) algorithms.

A. Signal Preprocessing Analysis

In this Section, the two-loop Kalman filtering algorithm proposed in this paper is analyzed with the original signal of the trainer performing the motion “single-arm rowing.”

Fig. 6 shows the comparison between the original signal and the signal after data stream filtering. The original signal data are smoother after data stream filtering, and the measurement noise is well suppressed. A no-action time of about 3 s

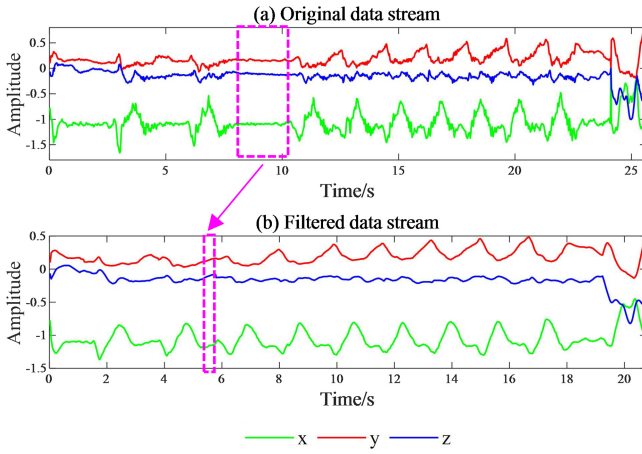


Fig. 6. The original data stream and the filtered data stream.

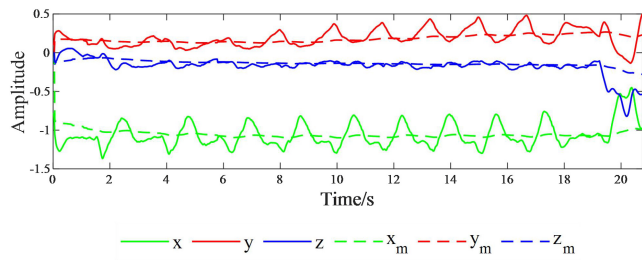


Fig. 7. The signal numerical filtering and real-time mean value.

after the completion of the second motion cycle is observed, during which about 150 points of uninformative interference data measured are directly removed when data stream filtering is performed. This result shows that the first-loop Kalman filtering can effectively separate the high-frequency signals, and the main components of the motion obtained from the separated sensor measurements. Moreover, the uninformative signals are not counted in the information stream, reducing the information storage requirements for the MEMS and the overall system power consumption during user rest.

The second-loop Kalman filter is used to extract the real-time mean value of the signal, and the results are shown in Fig. 6. The dashed line is the real-time mean value generated by the second-permutation Kalman filter. The second-loop Kalman filter can effectively extract the trend of the signal. When the signal undergoes large fluctuations (rapid fluctuations of the signal after the horizontal coordinate 900 in Fig. 7), the second-loop Kalman filter can effectively track and extract the fluctuating mean trend of the signal in time. It can be combined with the subsequent pseudo-periodic feature motion segmentation.

First- and second-loop Kalman filtering are combined to obtain the filtered, de-invalidated information, and trended temporal signals, as shown in Fig. 8. The peak value of the signal extracted automatically by applying the peak identification algorithm mentioned in the second part of Section III is also plotted together. Moreover, the signal between each peak value of the signal extracted according to this method contains the information of the user performing one motion. However, the peak (valley) value of the acceleration criterion point occurs at the process point where the direction

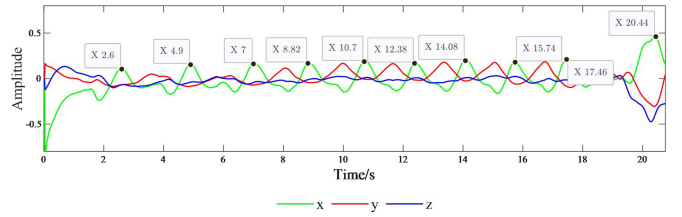


Fig. 8. De-trend the peak of the signal.

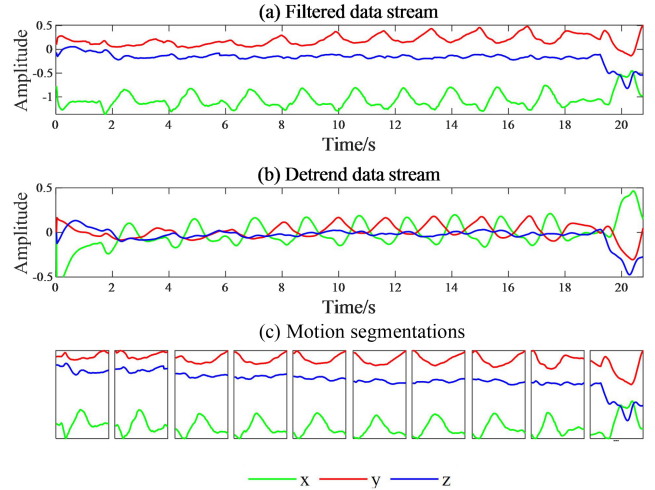


Fig. 9. De-trending signal acquisition and motion segmentation.

of the dumbbell movement turns, which is the middle point of the whole dumbbell movement cycle. To obtain the complete dumbbell movement cycle, the actual splitting point is the midpoint of the two adjacent criterion points.

B. Motion Segmentation Effect Analysis

In this Section, the original signal of the coach's motion "single-arm rowing" is also taken as an example to show the effect of the two-loop Kalman filter motion segmentation algorithm proposed in this paper. The segmentation of the motion segmentation algorithm is obtained from the detrended signal, but the motion signal is segmented based on the output result of the first-loop Kalman filter. Fig. 9 shows the result of the motion segment after segmentation. The motion segmentation is effective.

TABLE III describes the motion segmentation. Except that the red mark indicates that the motion segmentation is inaccurate in the later manual verification, the additional identification part is the noise content, the black mark is the effective motion segmentation, and the additional identification part is one more motion in the test. The average accuracy of overall segmentation is 98.33%.

C. Essential Experimental Details

In the previous subsection, 472 motion data segments are divided. After manual processing and cleaning, 455 valid data segments are retained and used as the dataset. In training, 60% of the data is used for the model training, 20% is used as the validation set for model parameter setting, and 20% is used

TABLE III
MOTION SPLIT RECORD

Segmentation	M1	M2	M3	M4	M5	M6	Acc %
Coach	10	11	10	10	10	10	98.4
Person 1	10	10	10	10	8	10	96.7
Person 2	10	11	4	10	11	11	95.0
Person 3	10	10	9	10	11	11	98.4
Person 4	10	10	10	11	10	10	98.4
Person 5	10	11	10	10	3	11	91.7
Person 6	10	10	6	10	11	10	95.0
Person 7	10	10	10	10	11	11	96.8
Acc %	100	96.4	86.3	98.8	93.8	96.3	98.3

TABLE IV
MOTION CLASSIFICATION ACCURACY

Methods\ Accuracy%	M1	M2	M3	M4	M5	M6	Avg
NB	85.7	100	100	94.1	100	100	96.7
SVM	100	100	100	90.0	93.8	100	96.7
KNN	100	100	100	90.0	93.8	100	96.7
NN	100	100	100	94.7	100	100	98.9

TABLE V
MOTION POSTURE ACCURACY SCORING

Methods\ Accuracy%	Bad	Good	Perfect	Avg.
NB	32.0	64.7	71.4	59.3
SVM	39.3	75.0	88.6	69.2
KNN	78.6	79.4	95.4	86.8
NN	73.7	88.5	95.7	89.0

as the test set to verify the model results. In the validation set, the learning rate of the final model is selected as 0.02, and the dropout rate is 0.5, the optimizer is Adam optimizer, the number of training iterations is 2000, and the size of the minibatch is 41–40 to ensure that the complete training set is traversed every 10 iterations.

D. Comparison and Analysis of Results

The classification and accuracy analysis of the motions are compared with the Naive Bayesian (NB), SVM, and KNN algorithms. The three methods are trained using the same training set as NNs and tested using the same test set.

TABLE IV below shows the classification accuracy score results of the three commonly used classification methods and the NN method on the test set. The NN method achieves the best accuracy in classification accuracy for all six motions. Hence, the NN method can effectively perform the classification counting of the motions.

TABLE IV shows the results of the three commonly used classification methods and NN methods for motion pose accuracy scoring on the test set, and NN achieves the best results. The advantage is evident compared with the NB method and SVM, indicating that the NN method has greater generalizability for the same data set size.

TABLE V shows the results of the three commonly used classification methods and NN methods for motion pose accuracy scoring on the test set, and NN achieves the best results. The advantage is evident compared with the NB and SVM,

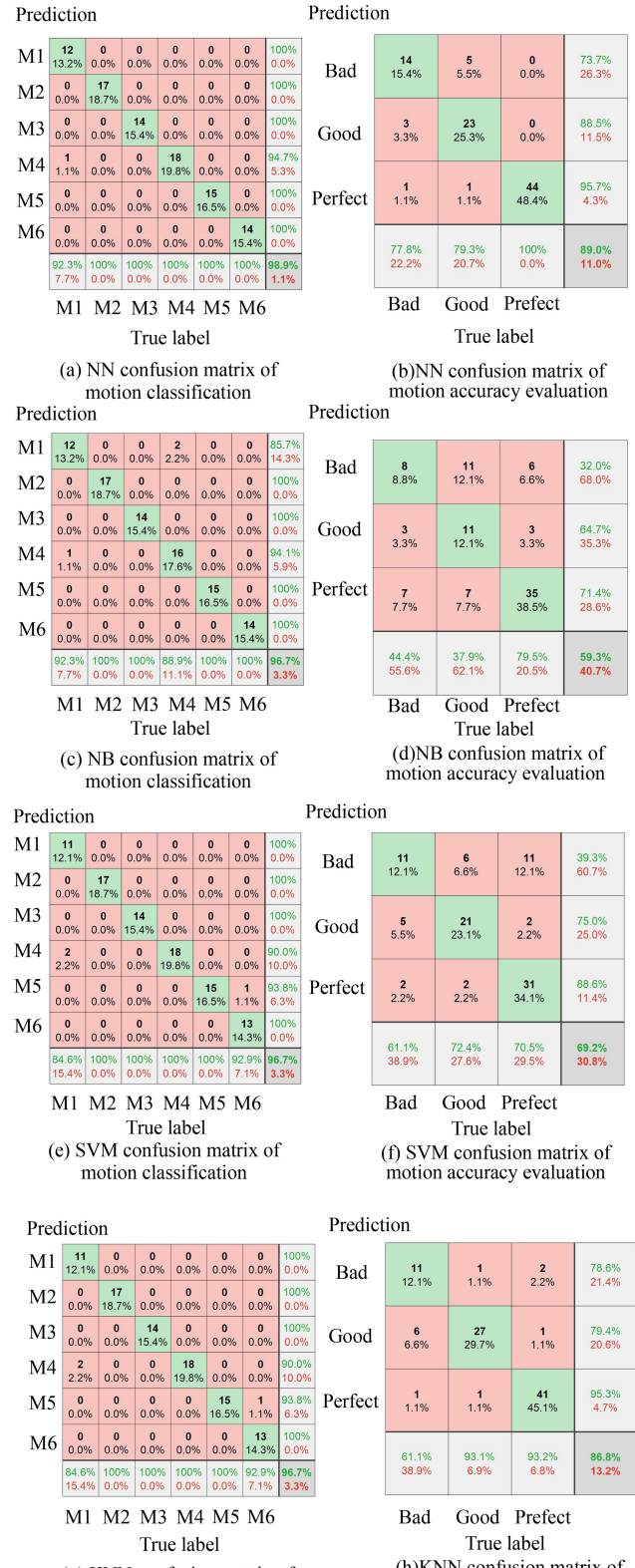


Fig. 10. Confusion matrix based on neural networks and other comparison methods on the test set.

indicating that the NN method has greater generalizability for the same data set size.

The confusion matrix of motion classification and motion posture diagnosis is shown in Fig. 10. We established

confusion matrices for motion category division and motion accuracy description and compared our proposed NN algorithm with conventional classification algorithms such as NB, SVM, and KNN. The NB algorithm can handle both continuous and categorical data, but it has a weakness in handling nonlinear relationships. The SVM can be used for both classification and regressions, but it needs to select kernel functions and hyperparameters. The KNN algorithm can work well with small datasets but it is sensitive to irrelevant features which makes the cost of computational power. For the classification of motion categories, we used the previous six action categories of M1-M6, and for the description of action accuracy, we established three evaluation indicators: bad, good and perfect. It can be seen from Figure 10 that in the classification of motion categories, the NN algorithm can achieve an accuracy rate of 98.9%, while NB, SVM and KNN can only achieve an accuracy rate of 96.7%, respectively. Similarly, in terms of motion accuracy evaluation, the accuracy rate of NN can reach 89%, while NB, SVM and KNN are 59.3%, 69.2% and 86.8% respectively. To sum up, the proposed NN algorithm is superior to the other three algorithms in terms of the classification of action categories and the description of action accuracy. The analysis of classification results shows that although the NN used has a simple structure, it can effectively realize the classification and analysis of motions. From the perspective of pose analysis accuracy, the output results of the NN used in the “Bad” category are relatively inaccurate, and 26% of the “Bad” motion segments predicted by the network are good, but the prediction of the “Perfect” category is very accurate.

V. CONCLUSION

This paper focuses on designing the experimental scheme, data acquisition, and data processing algorithm using MEMS technology in the smart dumbbell. The MEMS data acquisition system enables motion segmentation and information transmission. A mobile app on the user terminal recognizes and analyzes the movements and uploads the data to the cloud for summary analysis. The designed data flow filtering and segmentation algorithms based on axial acceleration signals from the MEMS sensor achieve signal smoothing, detrend signal acquisition, and pseudo periodic motion segmentation with high accuracy (98.8%). The proposed system effectively classifies dumbbell motions and diagnoses postures, demonstrating practical value. Future research will focus on enhancing method robustness and extending it to various sports beyond dumbbells.

REFERENCES

- [1] I.-M. Lee, E. J. Shiroma, F. Lobelo, P. Puska, S. N. Blair, and P. T. Katzmarzyk, “Effect of physical inactivity on major non-communicable diseases worldwide: An analysis of burden of disease and life expectancy,” *Lancet*, vol. 380, no. 9838, pp. 219–229, 2012.
- [2] M. P. Herring, P. J. O’Connor, and R. K. Dishman, “The effect of exercise training on anxiety symptoms among patients: A systematic review,” *Arch. Intern. Med.*, vol. 170, no. 4, pp. 321–331, 2010.
- [3] Y. Zhou, C. Xie, S. Sun, X. Zhang, and Y. Wang, “A self-supervised human activity recognition approach via body sensor networks in smart city,” *IEEE Sensors J.*, early access, Jun. 8, 2023, doi: [10.1109/JSEN.2023.3282601](https://doi.org/10.1109/JSEN.2023.3282601).
- [4] J. Taborri et al., “Sport biomechanics applications using inertial, force, and EMG sensors: A literature overview,” *Appl. Bionics Biomech.*, vol. 2020, 2020, Art. no. 2041549.
- [5] Y. Zhou, Z. Yang, X. Zhang, and Y. Wang, “A hybrid attention-based deep neural network for simultaneous multi-sensor pruning and human activity recognition,” *IEEE Internet Things J.*, vol. 9, no. 24, pp. 25363–25372, Dec. 2022.
- [6] D. Arsenault and A. D. Whitehead, “Gesture recognition using Markov systems and wearable wireless inertial sensors,” *IEEE Trans. Consum. Electron.*, vol. 61, no. 4, pp. 429–437, Nov. 2015, doi: [10.1109/TCE.2015.7389796](https://doi.org/10.1109/TCE.2015.7389796).
- [7] M. Al-Hammadi, G. Muhammad, W. Abdul, M. Alsulaiman, and M. S. Hossain, “Hand gesture recognition using 3D-CNN model,” *IEEE Consum. Electron. Mag.*, vol. 9, no. 1, pp. 95–101, Jan. 2020, doi: [10.1109/MCE.2019.2941464](https://doi.org/10.1109/MCE.2019.2941464).
- [8] M. Panella and R. Altilio, “A smartphone-based application using machine learning for gesture recognition: Using feature extraction and template matching via hu image moments to recognize gestures,” *IEEE Consum. Electron. Mag.*, vol. 8, no. 1, pp. 25–29, Jan. 2019, doi: [10.1109/MCE.2018.2868109](https://doi.org/10.1109/MCE.2018.2868109).
- [9] D. Ayata, Y. Yaslan, and M. E. Kamasak, “Emotion based music recommendation system using wearable physiological sensors,” *IEEE Trans. Consum. Electron.*, vol. 64, no. 2, pp. 196–203, May 2018, doi: [10.1109/TCE.2018.2844736](https://doi.org/10.1109/TCE.2018.2844736).
- [10] B. Mortazavi, S. Nyamathi, S. I. Lee, T. Wilkerson, H. Ghasemzadeh, and M. Sarrafzadeh, “Near-realistic mobile Exergames with wireless wearable sensors,” *IEEE J. Biomed. Health Inform.*, vol. 18, no. 2, pp. 449–456, Mar. 2014, doi: [10.1109/JBHI.2013.2293674](https://doi.org/10.1109/JBHI.2013.2293674).
- [11] A. Smerdov, A. Somov, E. Burnaev, B. Zhou, and P. Lukowicz, “Detecting video game player burnout with the use of sensor data and machine learning,” *IEEE Internet Things J.*, vol. 8, no. 22, pp. 16680–16691, Nov. 2021.
- [12] R. Dizon-Paradis, R. R. Kalavakonda, P. Chakraborty, and S. Bhunia, “Pasteables: A flexible and smart “stick-and-peel” wearable platform for fitness & athletics,” *IEEE Consum. Electron. Mag.*, early access, Mar. 9, 2022, doi: [10.1109/MCE.2022.3158044](https://doi.org/10.1109/MCE.2022.3158044).
- [13] Y. Huang and Y. Bai, “Intelligent sports prediction analysis system based on edge computing of particle swarm optimization algorithm,” *IEEE Consum. Electron. Mag.*, vol. 12, no. 2, pp. 73–82, Mar. 2023, doi: [10.1109/MCE.2021.3139837](https://doi.org/10.1109/MCE.2021.3139837).
- [14] S. Ganzevles, R. Vullings, P. J. Beek, H. Daanen, and M. Truijens, “Using tri-axial accelerometry in daily elite swim training practice,” *Sensors*, vol. 17, no. 5, p. 990, 2017.
- [15] Z. Wang et al., “Using wearable sensors to capture posture of the human lumbar spine in competitive swimming,” *IEEE Trans. HumanMach. Syst.*, vol. 49, no. 2, pp. 194–205, Apr. 2019.
- [16] F. Dadashi, F. Crettenand, G. P. Millet, L. Seifert, J. Komar, and K. Aminian, “Automatic front-crawl temporal phase detection using adaptive filtering of inertial signals,” *J. Sports Sci.*, vol. 31, no. 11, pp. 1251–1260, 2013.
- [17] A. Sharma, Y. Shah, Y. Agrawal, and P. Jain, “iYogacare: Real-time yoga recognition and self-correction for smart healthcare,” *IEEE Consum. Electron. Mag.*, vol. 12, no. 4, pp. 47–52, 2023, doi: [10.1109/MCE.2022.3171054](https://doi.org/10.1109/MCE.2022.3171054).
- [18] A. Bulling, U. Blanke, and B. Schiele, “A tutorial on human activity recognition using body-worn inertial sensors,” *ACM Comput. Surveys*, vol. 46, no. 3, pp. 1–33, 2014.
- [19] D. M. Burns, N. Leung, M. Hardisty, C. M. Whyne, P. Henry, and S. McLachlin, “Shoulder physiotherapy exercise recognition: Machine learning the inertial signals from a smartwatch,” *Physiol. Meas.*, vol. 39, no. 7, 2018, Art. no. 075007, doi: [10.1088/1361-6579/aacf9](https://doi.org/10.1088/1361-6579/aacf9).
- [20] A. Kos and A. Umek, “Wearable sensor devices for prevention and rehabilitation in healthcare: Swimming exercise with real-time therapist feedback,” *IEEE Internet Things J.*, vol. 6, no. 2, pp. 1331–1341, Apr. 2019.
- [21] Y.-L. Hsu, H.-C. Chang, and Y.-J. Chiu, “Wearable sport activity classification based on deep convolutional neural network,” *IEEE Access*, vol. 7, pp. 170199–170212, 2019.
- [22] X. Sha et al., “Accurate recognition of player identity and stroke performance in table tennis using a smart wristband,” *IEEE Sensors J.*, vol. 21, no. 9, pp. 10923–10932, May 2021.
- [23] D. Ravi, C. Wong, B. Lo, and G.-Z. Yang, “A deep learning approach to on-node sensor data analytics for mobile or wearable devices,” *IEEE J. Biomed. Health Inform.*, vol. 21, no. 1, pp. 56–64, Jan. 2017.
- [24] F. Gu, M.-H. Chung, M. Chignell, S. Valaee, B. Zhou, and X. Liu, “A survey on deep learning for human activity recognition,” *ACM Comput. Surveys*, vol. 54, no. 8, pp. 1–34, 2021.

- [25] K. Xia, H. Wang, M. Xu, Z. Li, S. He, and Y. Tang, "Racquet sports recognition using a hybrid clustering model learned from integrated wearable sensor," *Sensors*, vol. 20, no. 6, p. 1638, 2020.
- [26] T. T. Alemayoh, J. H. Lee, and S. Okamoto, "New sensor data structuring for deeper feature extraction in human activity recognition," *Sensors*, vol. 21, no. 8, p. 2814, 2021.
- [27] J. Ma, L. Sun, H. Wang, Y. Zhang, and U. Aickelin, "Supervised anomaly detection in uncertain pseudoperiodic data streams," *ACM Trans. Internet Technol. (TOIT)*, vol. 16, no. 1, pp. 1–20, 2016.
- [28] X. Hu, X. Bao, S. Xie, and G. Wei, "Unsupervised motion capture data segmentation based on topic model," *Comput. Animat. Virtual Worlds*, vol. 32, nos. 3-4, p. e2005, 2021.
- [29] L.-A. Tang, B. Cui, H. Li, G. Miao, D. Yang, and X. Zhou, "Effective variation management for pseudo periodical streams," in *Proc. 2007 ACM SIGMOD Int. Conf. Manage. Data*, 2007, pp. 257–268.
- [30] Y. Wang, M. Chen, X. Wang, R. H. Chan, and W. J. Li, "IoT for next-generation racket sports training," *IEEE Internet Things J.*, vol. 5, no. 6, pp. 4558–4566, Dec. 2018.
- [31] Y. Wang, Y. Zhao, R. H. Chan, and W. J. Li, "Volleyball skill assessment using a single wearable micro inertial measurement unit at wrist," *IEEE Access*, vol. 6, pp. 13758–13765, 2018.
- [32] S. Lu, X. Zhang, J. Wang, Y. Wang, M. Fan, and Y. Zhou, "An IoT-based motion tracking system for next-generation foot-related sports training and talent selection," *J. Healthc. Eng.*, vol. 2021, 2021, Art. no. 9958256, doi: [10.1155/2021/9958256](https://doi.org/10.1155/2021/9958256).
- [33] L. L. Andersen, C. H. Andersen, O. S. Mortensen, O. M. Poulsen, I. B. T. Bjørnlund, and M. K. Zebis, "Muscle activation and perceived loading during rehabilitation exercises: Comparison of dumbbells and elastic resistance," *Physical Therapy*, vol. 90, no. 4, pp. 538–549, 2010, doi: [10.2522/ptj.20090167](https://doi.org/10.2522/ptj.20090167).
- [34] H. Sakoe and S. Chiba, "Dynamic programming algorithm optimization for spoken word recognition," *IEEE Trans. Signal Process.*, vol. 26, no. 1, pp. 43–49, Feb. 1978.



Haodong Huang was born in Jingmen, China. He received the B.S. degree in mechanical engineering from the School of Mechanical Engineering and Automation, University of Northeast of China, China in 2021. He is currently pursuing the M.S. degree in mechanical engineering with the School of Mechanical Engineering and Automation, Harbin Institute of Technology (Shenzhen), Shenzhen. His research interests include mechanical fault diagnosis and condition monitoring.



Yufan Wang (Member, IEEE) received the B.S. degree in communications engineering from Beijing Jiaotong University, Beijing, China, in 2014, and the Ph.D. degree from the City University of Hong Kong, Hong Kong, in 2018. He is currently a Postdoctoral Researcher with the Department of Industrial Engineering and Management, School of Mechanical Engineering, Shanghai Jiao Tong University, Shanghai, China. His current research interests include wearable cyber-physical devices, inertial measurement units, artificial intelligence, and sports motion analysis.



Shilong Sun (Member, IEEE) received the Ph.D. degree from the City University of Hong Kong in 2018.

He is currently an Assistant Professor with the Harbin Institute of Technology (Shenzhen), Shenzhen, China. He nurtures keen interests in vibration energy harvesting design, fault diagnosis and prognosis, decision-making with artificial intelligence, and deep learning for industrial data. He currently focuses on the remaining equipment life estimation research with deep learning and smart energy harvesting techniques.



Xiao Zhang (Member, IEEE) received the B.Eng. and M.Eng. degrees from South-Central Minzu University, Wuhan, China, in 2009 and 2011, respectively, and the Ph.D. degree from the Department of Computer Science, City University of Hong Kong, Hong Kong, in 2016. In 2015, he was a Visiting Scholar with Utah State University, Utah, USA. From 2016 to 2019, he was a Postdoctoral Research Fellow with the Singapore University of Technology and Design. He is currently an Associate Professor with the College of Computer Science, South-Central Minzu University. His research interests include algorithms design and analysis, edge computing, wireless, and UAV networking.



Tengyi Peng was born in Shaoguan, China. He received the B.S. degree in mechanical design manufacture and automation from the School of Mechanical and Electrical Engineering, University of Electronic Science and Technology of China, China, in 2020. He is currently pursuing the M.S. degree in mechanical engineering with the School of Mechanical Engineering and Automation, Harbin Institute of Technology (Shenzhen), Shenzhen. His research interests include mechanical fault diagnosis and condition monitoring.



Yu Zhou (Member, IEEE) received the B.Sc. degree in electronics and information engineering and the M.Sc. degree in circuits and systems from Xidian University, Xi'an, China, in 2009 and 2012, respectively, and the Ph.D. degree in computer science from the City University of Hong Kong, Hong Kong, in 2017. He is currently a Tenured Associate Professor with the College of Computer Science and Software Engineering, Shenzhen University, Shenzhen, China. His current research interests include computational intelligence, machine learning, and intelligent information processing.